

## An X-band GaN combined solid-state power amplifier\*

Chen Chi(陈炽)<sup>†</sup>, Hao Yue(郝跃), Feng Hui(冯辉), Yang Linan(杨林安), Ma Xiaohua(马晓华),  
Duan Huantao(段焕涛), and Hu Shigang(胡仕刚)

(Key Laboratory of Wide Band-Gap Semiconductor Materials and Device, School of Microelectronics,  
Xidian University, Xi'an 710071, China)

**Abstract:** Based on a self-developed AlGaIn/GaN HEMT with 2.5 mm gate width technology on a SiC substrate, an X-band GaN combined solid-state power amplifier module is fabricated. The module consists of an AlGaIn/GaN HEMT, Wilkinson power couplers, DC-bias circuit and microstrip line. For each amplifier, we use a bipolar DC power source. Special RC networks at the input and output and a resistor between the DC power source and the gate of the transistor at the input are used for cancellation of self-oscillation and crosstalk of low-frequency of each amplifier. At the same time, branches of length  $3\lambda/4$  for Wilkinson power couplers are designed for the elimination of self-oscillation of the two amplifiers. Microstrip stub lines are used for input matching and output matching. Under  $V_{ds} = 27$  V,  $V_{gs} = -4.0$  V, CW operating conditions at 8 GHz, the amplifier module exhibits a line gain of 5.6 dB with power added efficiency of 23.4%, and output power of 41.46 dBm (14 W), and the power gain compression is 3 dB. Between 8 and 8.5 GHz, the variation of output power is less than 1.5 dB.

**Key words:** AlGaIn/GaN HEMT; solid-state power amplifiers; output power; gain compression; power added efficiency

**DOI:** 10.1088/1674-4926/30/9/095001

**PACC:** 7280; 7280E

**EEACC:**1350F; 2560P; 1350H

### 1. Introduction

In radar and broadcast communication applications, T/R components are key elements. Inside these T/R components, the high-power amplifier is the one of the most important microwave modules. At high frequencies, high power amplifiers are based on the GaAs PHEMT, MESFET and HBT transistors. However, due to the thermal and electrical limitations of GaAs transistors, they cannot meet future system requirements. For the demands of amplifiers, wide band gap semiconductors emerge as the first choice. In these, the AlGaIn/GaN high electron mobility transistor (AlGaIn/GaN HEMT) is very attractive for power application because of its high breakdown voltage, high carrier density, high saturation velocity and excellent thermal conductivity of the SiC substrate<sup>[1,2]</sup>. In recent years, there have been several reports on the high signal performance of AlGaIn/GaN HEMTs as discrete devices with very high output power densities. Wu *et al.*<sup>[3]</sup> designed an AlGaIn/GaN HEMT with field plate technology in the X band. The operation voltage is 120 V and CW output power density is 30.6 W/mm. In 2006, Takagi<sup>[4]</sup> reported an AlGaIn/GaN HEMT with gate-width 11.52 mm, and at 9.5 GHz, CW output power is 81.3 W. This is the highest power in the GaN power transistor in the X band.

With the development of material growth and device fabrication technology, GaN-based amplifiers have attracted a growing interest among the research community. AlGaIn/GaN HEMT MMICs have been widely reported<sup>[5-8]</sup>. Recently, Piotrowicz<sup>[9]</sup> implemented a state-of-the-art GaN MMIC am-

plifier with a size of 18 mm<sup>2</sup>, whose output power reached 58 W. This result is the highest level achieved in GaN-based power MMIC amplifiers.

Compared to internal-matched HEMT devices and MMIC amplifiers, the solid-state power amplifier (SSPA) can support higher power, better reliability, and longer run time. But there are few reports on the GaN solid-state amplifier in the development of GaN-based circuits<sup>[10]</sup>. In this paper, based on a self-developed AlGaIn/GaN HEMT with 2.5 mm gate width technology on a SiC substrate<sup>[11]</sup>, with microstrip matching technology and load pull measurement by adjusting the microstrip stub line, we design and fabricate a two-way combined solid-state amplifier. To avoid the instability of the SSPA, we use a  $3\lambda/4$  separated branch transformer, RC stable networks and resistors between the DC power source and the gate of the transistor. Under  $V_{ds} = 27$  V and  $V_{gs} = -4.0$  V CW operating conditions at 8 GHz, the developed two-way combined solid-state amplifier with two 2.5 mm gate width AlGaIn/GaN HEMTs demonstrated an output power of 41.46 dBm with power added efficiency of 23.4% and a power combining efficiency of 82.3%.

### 2. Device technology

The sample was grown by low-pressure MOCVD on a 4H-SiC substrate. Hydrogen was used as the carrier gas. Triethylgallium (TEGa), trimethylaluminum (TMAI) and ammonia (NH<sub>3</sub>) were used as precursors. Prior to the epitaxial growth, the 4H-SiC substrate was annealed at 1050 °C for

\* Project supported by the National Natural Science Foundation of China (Nos. 60736033, 60676048).

<sup>†</sup> Corresponding author. Email: ccachi@163.com

Received 1 April 2009

© 2009 Chinese Institute of Electronics

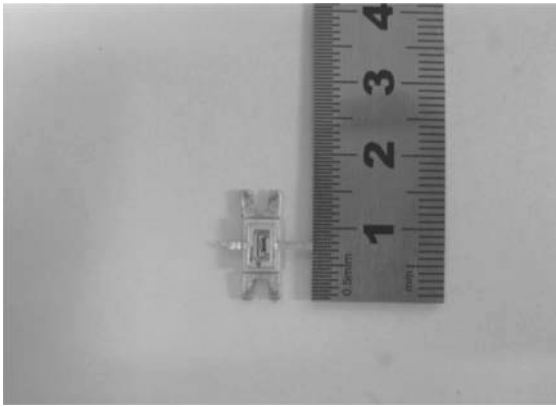


Fig. 1. External view of the GaN power HEMT.

10 min in order to remove surface contamination. A 100 nm thick high-temperature (HT) AlN nucleation layer was deposited at 1100 °C. Then, the susceptor temperature was decreased to 1020 °C and a 2 μm thick GaN buffer layer was grown, followed by a 24 nm thick undoped AlGaN barrier layer. The reactor pressure was kept at 40 Torr during the growth. The Al component was 30% in the AlGaN layer. A sheet resistance of 308 Ω/□, room temperature mobility of 1570 cm<sup>2</sup>/(V·s), and sheet carrier concentration of 1.29 × 10<sup>13</sup> cm<sup>-2</sup> were measured respectively. The device process followed standard HEMT processing technology. Device isolation was accomplished by Cl<sub>2</sub>-based dry etching with an etching depth of about 150 nm, Ti/Al/Ni/Au (20 nm/120 nm/55 nm/45 nm) ohmic contact deposition was formed by electron-beam evaporation and annealing at 850 °C for 30 s, while Ni/Au (20 nm/200 nm) was utilized as the Schottky gate. After all the device processes, the SiN passivation layer was deposited by employing PECVD and a device with a gate length of 0.4 μm and a gate width of 20 × 125 μm demonstrated an average saturation current of 2 A/mm at a gate voltage of 1 V. The pinch-off voltage was -4.7 V. The packaged GaN high power transistor is shown in Fig. 1.

### 3. Solid-state amplifier design

#### 3.1. Circuit design of the two-way combined GaN-based SSPA

The configuration of the two-way Wilkinson combined amplifiers is shown in Fig. 2. The two-way combined SSPA is fabricated on the substrate by the microwave material division of Rogers Corporation and the substrates have a relative dielectric constant of 2.94, height of 0.78 mm and metallization copper thickness of 0.018 mm. The amplifier module consists of the 3 dB Wilkinson couplers, input matching circuit, output matching circuit and DC-biased circuit. The two identical amplifiers are connected in parallel through Wilkinson couplers, which operate as a power divider at the input and a power combiner at the output, respectively.

In Fig. 2, for each amplifier, we use the bipolar DC power source. In Fig. 2, the characteristic impedances of Z<sub>1</sub>, Z<sub>3</sub> are 128 Ω, and those of Z<sub>2</sub>, Z<sub>4</sub> are 109 Ω. The length is 1/4 microstrip wavelength. The radial stubs are open to the

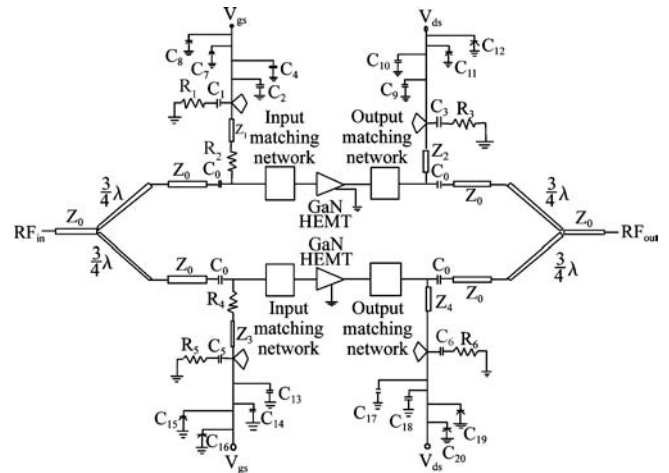


Fig. 2. Schematic diagram of the GaN-based two-way combined amplifier.

odd harmonious waves and they are short to the even harmonious waves, which is useful for preventing leakage of energy from the bias network. We then eliminated the even harmonious waves and kept all the odd harmonious waves, which is helpful for promoting the linearity and output power of the amplifier<sup>[12]</sup>. At the same time, the radial stubs can improve the microwave performance of the power device in output power and gain<sup>[13]</sup>. C<sub>2</sub>, C<sub>4</sub>, C<sub>9</sub>, C<sub>10</sub>, C<sub>13</sub>, C<sub>14</sub>, C<sub>17</sub> and C<sub>18</sub> are decoupling capacitances filtering the noise from the DC power, and C<sub>7</sub>, C<sub>8</sub>, C<sub>11</sub>, C<sub>12</sub>, C<sub>15</sub>, C<sub>16</sub>, C<sub>19</sub> and C<sub>20</sub> can prevent the interference of the low-frequency RF signal to the DC power. C<sub>0</sub> is an RF single coupling capacitance, which can isolate the DC current. Because of the large DC current, the drain DC supply wire is thicker than that of the gate DC supply.

On the other hand, because the power transistor is a large periphery device without internal matching, the external matching circuit is mainly based on the large signal test by changing the length and width of the microstrip stub at the input and output.

#### 3.2. Wilkinson power divider/combiner

The two-way Wilkinson divider/combiner has the advantages of simple construction and high port-to-port isolation<sup>[14]</sup>. As is well known, the 3 dB Wilkinson couplers are power equal-split networks and they can be made to have all ports matched with isolation between the output ports. No power is dissipated by the resistor when the output ports are matched. However, if a reflection occurs at one of the output terminals, the reflected signal will split, and through the different paths of λ/2, they can completely cancel at the remaining output terminal<sup>[15]</sup>.

However, in our design, we use the 3λ/4 for the branch couple rather than the traditional λ/4, as shown in Fig. 3. This is because in the X-band, the electrical length of 90° of output branches of the standard symmetrical Wilkinson must be placed very close to each other for connecting the surface mounted resistor. This will give rise to strong mutual coupling between the output lines<sup>[16]</sup> and during the measurement, we found the traditional λ/4 Wilkinson power divider/combiner

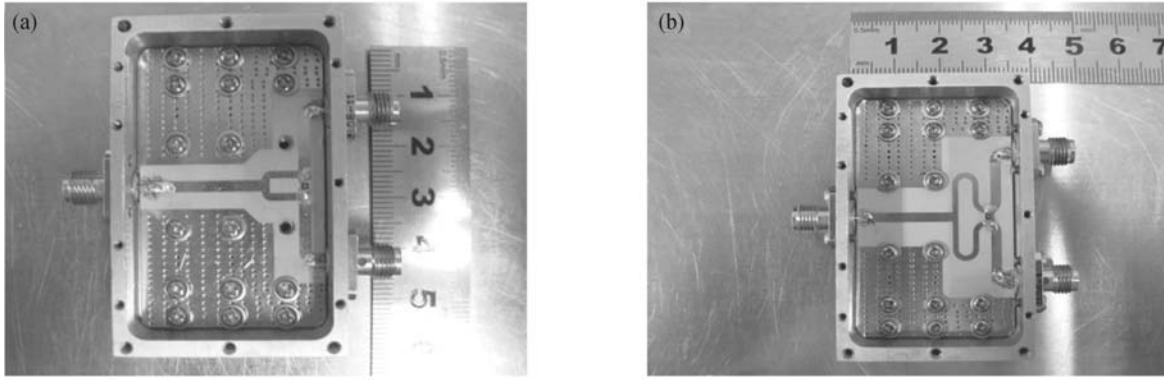


Fig. 3. Internal view of the (a)  $\lambda/4$  and (b)  $3\lambda/4$  Wilkinson power divider.

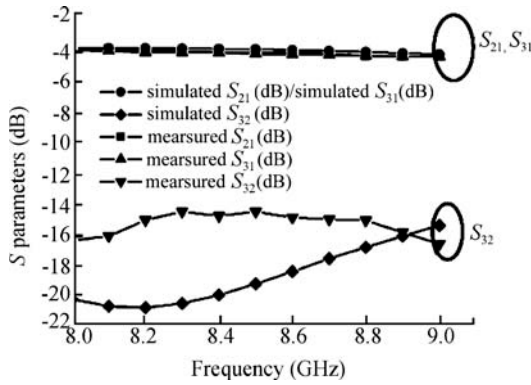


Fig. 4. Simulated and measured insertion loss and isolation.

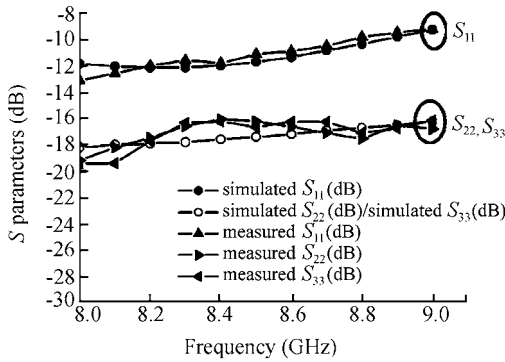


Fig. 5. Simulated and measured return loss at the input and output ports.

can cause serious self-oscillation when used in a combined amplifier. However, the Wilkinson power divider and combiner which have semicircular  $3\lambda/4$  arms can separate the branches widely and eliminate self-oscillation effectively.

The simulated and measured insertion loss and isolation of the  $3\lambda/4$  microstrip branch are plotted in Fig. 4. The simulated and measured return losses are plotted in Fig. 5. Good agreement between simulation and measurement results of insertion loss ( $S_{21}$ ,  $S_{31}$ ) and return loss at input ( $S_{11}$ ) or at output ( $S_{22}$ ,  $S_{33}$ ) is observed. From Fig. 4, we know the the difference in power divided between the insertion loss of the two output ports is less than 0.2 dB from 8 to 9 GHz. From Fig. 5, the return loss at the input port is in the range of 10 and 12 dB across the band and the return loss at the output ports is between 16 and 20 dB in the same band. However, the isolation between the two output ports is around 16 dB in the

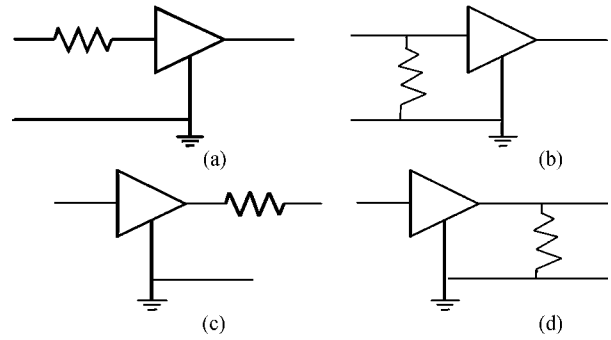


Fig. 6. Four types of resistive loading to improve stability<sup>[18]</sup>: (a) A series resistor at the input; (b) A shunt resistor at the input; (c) A series resistor at the output; (d) A shunt resistor at the output.

band, which is not in good agreement with simulated results. The difference is caused by two kinds of losses: division loss and microstrip radiation loss<sup>[17]</sup>, the latter being dominant.

### 3.3. Stability improvement of the SSPA

There are four ways to improve the stability of amplifier: using series or shunt resistors connected at the input or the output of the transistor (as shown in Fig. 6). Resistive loading at the input can deteriorate the noise performance of the amplifier<sup>[18]</sup>. But during the practical microwave tuning, to ensure the amplifier stable, the shunt resistor is a necessary part of circuit to make the amplifier stable.

In Fig. 2, the resistors ( $R_2$ ,  $R_4$ ) between the DC power and the gate of the transistor are used to improve stability and prevent self-oscillation of the amplifier. The shunt resistors  $R_3$  and  $R_6$  at the output can consume large DC power and reduce the power added efficiency dramatically. So, in order to reduce the total DC power consumption and protect the resistor R against a large current at the output, we select a configuration for stability improvement by a series capacitor  $C_3$ ,  $C_6$  to the shunt resistor. At the same time, we add RC ( $R_1$ ,  $C_1$  and  $R_5$ ,  $C_5$ ) stable networks at the input which have the same function as those at the output.

## 4. Experimental result

### 4.1. Large signal measurement system of the GaN HEMT SSPA

The system (as shown in Fig. 7) includes an HP8350B

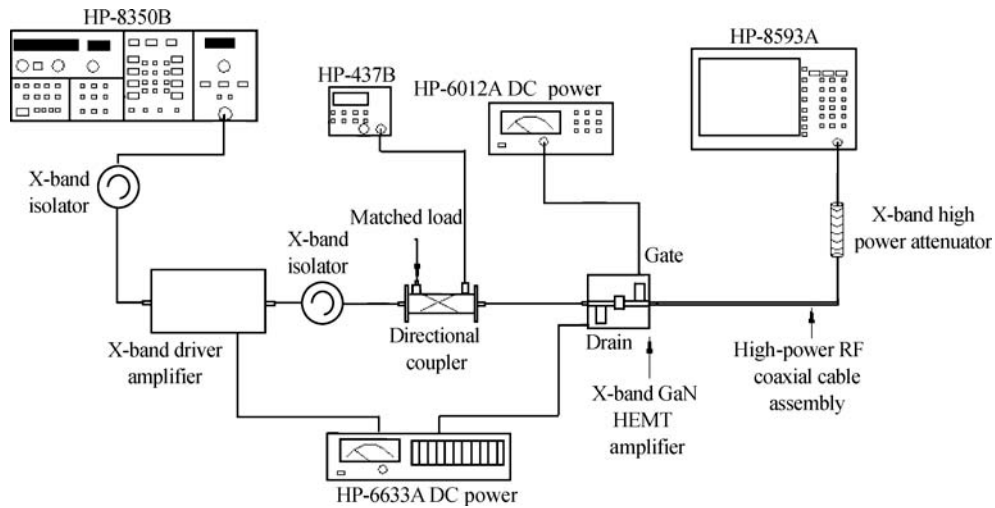


Fig. 7. Block diagram of the X band microwave measurement system.



Fig. 8. External view of the one-way GaN HEMT amplifier.

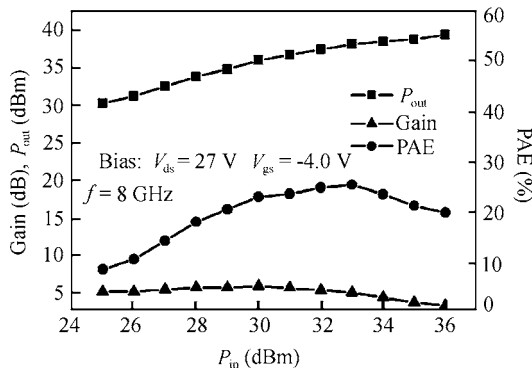


Fig. 9. Measured power performance of the one-way GaN HEMT SSPA at 8 GHz with  $V_{ds} = 27$  V and  $V_{gs} = -4.0$  V.  $P_{outmax} = 39.3$  dBm,  $PAE_{max} = 25.3\%$ .

sweep oscillator, HP437B power meter, HP8593A spectrum analyzer, four-way DC power, and the microwave measurement assembly. The driver amplifier can deliver an output power of 40 dBm in the X band.

#### 4.2. Large-signal performance of the one-way GaN HEMT amplifier

We also measured the single GaN HEMT amplifier under the same DC bias conditions. Figure 8 is an external view of the one-way GaN HEMT SSPA. Figure 9 shows the large signal measurements of the single transistor amplifier performed

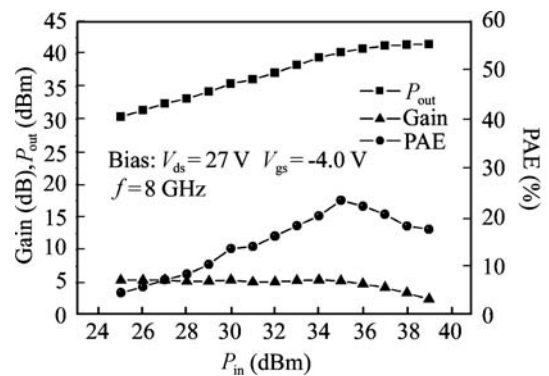


Fig. 10. Measured power performance of the two-way combined GaN HEMT SSPA at 8 GHz with  $V_{ds} = 27$  V and  $V_{gs} = -4.0$  V.  $P_{outmax} = 41.46$  dBm,  $PAE_{max} = 23.4\%$ .

at  $V_{ds} = 27$  V and  $V_{gs} = -4.0$  V. The largest linear gain is 5.9 dB. When the input power is 34 dBm, the output power is 38.4 dBm, and this corresponds to 1 dB gain compression with a total drain current of 726.5 mA. When the input power increases to 36 dBm, maximum output power of 39.3 dBm is achieved, with a drain current of 845.7 mA and the amplifier has 2 dB gain compression.

#### 4.3. Large-signal measurements of the two-way GaN HEMT SSPA

In Fig. 10, the large signal measurements of the two-way combined amplifier were performed when the drain bias voltage was 27 V and the gate bias voltage was  $-4.0$  V. The largest linear gain is 5.4 dB. When the input power is 36 dBm, the output power is 40.8 dBm, and this corresponds to a 1 dB gain compression with a total drain current of 1481.3 mA. When the input power increases to 39 dBm, a maximum output power of 41.46 dBm is achieved, with a drain current of 1657.2 mA and the amplifier has 3 dB gain compression. The maximum PAE of 23.4% is obtained at an input power of  $P_{in} = 35$  dBm. Because the one-way amplifier can deliver a maximum of 39.3 dBm at 8 GHz, the power combining efficiency is about 82.3%.

Figure 11 shows the dependence of output power and

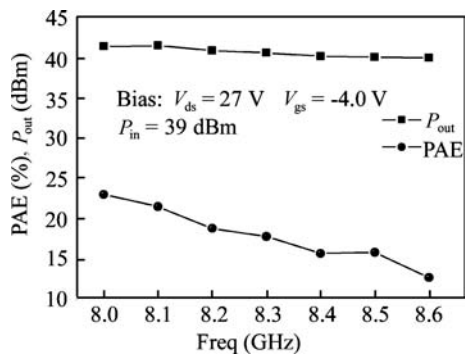


Fig. 11. Measured output power and PAE against frequency of the two-way combined GaN HEMT SSPA at  $P_{in} = 38$  dBm with  $V_{ds} = 27$  V and  $V_{gs} = -4.0$  V.

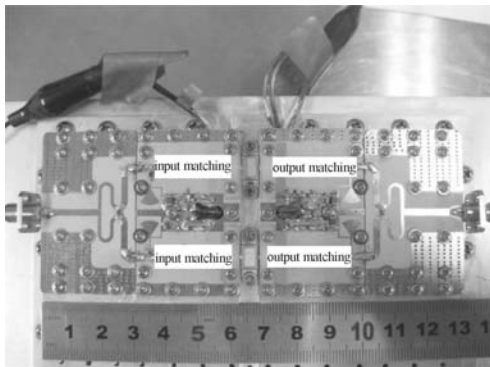


Fig. 12. Internal view of the two-way combined GaN HEMT SSPA.

PAE on frequency and the measurement condition is that drain voltage is 27 V and gate voltage is  $-4.0$  V. From the curve, we can see that the variation of output power between 8 and 8.5 GHz is less than 1.5 dB, with the maximum measured saturated output power of 41.5 dBm at 8.1 GHz and the minimum output power of 39.97 dBm at 8.5 GHz. The corresponding PAE varies from 23.2% at 8 GHz to 15.8% at 8.5 GHz. This is because the output power decreases with the variation of frequency and the drain current increases gradually with the variation of frequency. Figure 12 shows the internal view of the combined GaN HEMT solid-state amplifier.

## 5. Conclusion

A two-way combined GaN HEMT solid-state amplifier module was developed. Because of the potential instability of amplifiers, an RC stable network and a resistor which is between the DC power source and the gate of the transistor at input were designed to make the amplifier stable. In the design of the Wilkinson divider/combiner, in order to ensure the stability of the two-way amplifier,  $3\lambda/4$  transmission-lines were used to decrease the coupling of the microstrip. Under CW operating conditions at 8 GHz, the developed two-way combined solid-state amplifier delivered an output power 41.46 dBm with power added efficiency of 23.4% and a power com-

binning efficiency of 82.3% at  $V_{ds} = 27$  V,  $V_{gs} = -4.0$  V.

## References

- [1] Trew R J, Bilbro G L, Kuang W, et al. Microwave AlGaIn/GaN HFETs. *IEEE Microw Mag*, 2005, 6(1): 56
- [2] Mishra U K, Parikh P, Wu Y F. AlGaIn/GaN HEMTs—an overview of device operation and applications. *Proc IEEE*, 2002, 90(6): 1022
- [3] Wu Y F, Saxler A, Moore M, et al. 30-W mm GaN HEMTs by field plate optimization. *IEEE Electron Device Lett*, 2004, 25(3): 117
- [4] Takagi K, Masuda K, Kashiwabara Y, et al. X-band Al-GaN/GaN HEMT with over 80 W output power. *Compound Semiconductor Integrated Circuit Symposium*, 2006: 265
- [5] Schuh P, Leberer R, Sledzik H, et al. 20 W GaN HPAs for next generation X-band T R-modules. *Microwave Symposium Digest*, 2006: 726
- [6] Wurfl J, Behtash R, Lossy R, et al. Advances in GaN-based discrete power devices for L- and X-band applications. *Microwave Conference*, 2006: 1716
- [7] Moon J S, Wong D, Antcliffe M, et al. High PAE 1 mm Al-GaN/GaN HEMTs for 20 W and 43% PAE X-band MMIC amplifiers. *Electron Devices Meeting*, 2006: 1
- [8] Meliani C, Behtash R, Wurfl J, et al. A Broadband GaN-MMIC power amplifier for L to X bands. *Microwave Integrated Circuit Conference*, 2007: 147
- [9] Piotrowicz S, Morvan E, Aubry R, et al. State of the art 58 W, 38% PAE X-band AlGaIn/GaN HEMTs microstrip MMIC amplifiers. *Compound Semiconductor Integrated Circuits Symposium*, 2007: 1
- [10] Kanto K, Satomi A, Asahi Y, et al. An X-band 250 W solid-state power amplifier using GaN power HEMTs. *Radio and Wireless Symposium*, 2008: 77
- [11] Wang Chong, Hao Yue, Zhang Jincheng. Development and characteristics of AlGaIn/GaN HEMT. *Journal of Xidian University*, 2005, 32(2): 234 (in Chinese)
- [12] Chen Gaopeng, Chen Xiaojuan, Liu Xinyu, et al. A Ku band 30 W pulsed microwave power amplifier module. *Journal of Semiconductors*, 2008, 29(11): 2281 (in Chinese)
- [13] Luo Weijun, Chen Xiaojuan, Liang Xiaoxin, et al. A radial stub test circuit for microwave power devices. *Chinese Journal of Semiconductors*, 2006, 27(9): 1557
- [14] Chang K, Sun C. Millimeter-wave power-combining techniques. *IEEE Trans Microw Theory Tech*, 1983, 31(2): 91
- [15] Wilkinson E J. An N-way hybrid power divider. *IEEE Trans Microw Theory Tech*, 1960, 1: 116
- [16] Horst S, Bairavasubramanian R, Tentzeris M M, et al. Modified Wilkinson power dividers for millimeter-wave integrated circuits. *IEEE Trans Microw Theory Tech*, 2007, 55(11): 2439
- [17] Antsos D, Crist R, Sukamto L. A novel Wilkinson power divider with predictable performance at K and Ka-band. *Microwave Symposium Digest*, 1994, 5: 907
- [18] Gonzalez G. *Microwave transistor amplifiers analysis and design*. 2nd ed. New Jersey: Prentice Hall, 1997